RESEARCH PAPER

Tissue Barriers 2:4, e964547; September 1, 2014; © 2014 Taylor & Francis Group, LLC

Claudin-7, -16, and -19 during mouse kidney development

Halim Khairallah[1,†], Jasmine El Andalousi[2,†], Annie Simard[2,†], Nicholas Haddad[1], Yan-Hua Chen[3], Jianghui Hou[4], Aimee K Ryan[1,2,5,*], and Indra R Gupta[1,2,5,*]

[1]Department of Human Genetics; McGill University; Montreal, Quebec, Canada; [2]The Research Institute of the McGill University Health Center; Montreal Children's Hospital; Montreal, Quebec, Canada; [3]Department of Anatomy and Cell Biology; Brody School of Medicine at East Carolina University; Greenville, NC USA; [4]Washington University Renal Division; St. Louis, MO USA; [5]Department of Pediatrics; McGill University; Montreal, Quebec, Canada

[†]These authors contributed equally to this work.

[‡]Grant Sponsor: Kidney Foundation of Canada to PI A. K. Ryan and I. R. Gupta

Keywords: Loop of Henle, nephrogenesis, renal branching morphogenesis, tubule differentiation

Abbreviations: E, embryonic day; P, postnatal; FHHNC, familial hypomagnesaemia with hypercalciuria and nephrocalcinosis; nd, nephric duct; ub, ureteric bud; MET, mesenchymal to epithelial transition.

Members of the claudin family of tight junction proteins are critical for establishing epithelial barriers and for the regulation of paracellular transport. To understand their roles during kidney development, we first performed RT-PCR analyses and determined that 23 claudin family members were expressed in embryonic day (E) 13.5 mouse kidneys. Based on their developmental expression and phenotypes in mouse models, we hypothesized that 3 claudin members could affect nephron formation during kidney development. Using whole mount *in situ* hybridization and immunohistochemistry, we demonstrated that *Claudin-7* (*Cldn7*) was expressed in the nephric duct, the emerging ureteric bud, and in tubules derived from ureteric bud branching morphogenesis. In contrast, *Claudin-16* (*Cldn16*) and *Claudin-19* (*Cldn19*) were expressed at later stages of kidney development in immature renal tubules that become the Loop of Henle. To determine if a loss of these claudins would perturb kidney development, we examined newborn kidneys from mutant mouse models lacking *Cldn7* or *Cldn16*. In both models, we noted no evidence for any congenital renal malformation and quantification of nephron number did not reveal a decrease in nephron number when compared to wildtype littermates. In summary, *Cldn7*, *Cldn16,* and *Cldn19* are expressed in different epithelial lineages during kidney development. Mice lacking *Cldn7* or *Cldn16* do not have defects in *de novo* nephron formation, and this suggests that these claudins primarily function to regulate paracellular transport in the mature nephron.

Introduction

Members of the claudin family of integral membrane proteins are components of tight junctions: they connect adjacent epithelial cells to one another in a narrow band just beneath the apical surface to create an occluding seal.[1-2] Claudin proteins have well-established roles in renal, gastrointestinal, and lung physiology based on their abilities to regulate paracellular transport. However, many claudins are expressed during embryogenesis, suggesting that these proteins may also contribute to organ formation, including kidney development, through direct effects on cell adhesion, proliferation, and lumen formation.[3]

During mammalian kidney development, 2 primordial tissues, the ureteric bud and the metanephric mesenchyme, undergo epithelial morphogenesis to form the final metanephric kidney.[4] The kidneys and the ureters arise from 2 epithelial tubes that extend along the length of the embryo, the mesonephric ducts. An epithelial swelling emerges from the mesonephric duct at embryonic day (E) 10.5 during mouse embryonic development and is known as the ureteric bud. The ureteric bud invades the adjacent undifferentiated mesenchyme and induces the formation of the metanephric mesenchyme. Reciprocal signaling between the ureteric bud and the metanephric mesenchyme induces the ureteric bud to elongate and bifurcate in a process known as branching morphogenesis that ultimately gives rise to the collecting duct system of the adult kidney. The process of ureteric bud branching morphogenesis is critical for kidney development: each ureteric bud tip induces the adjacent metanephric mesenchyme to undergo mesenchymal-to-epithelial transition and this determines the final number of nephrons formed *in utero*. As part of mesenchymal-to-epithelial transition, a number of intermediate structures form including mesenchymal condensates, comma-shaped structures, S-shaped structures, and early and late tubules that eventually give rise to all of the nephron segments except the collecting duct.

*Correspondence to: Aimee K Ryan; Email: aimee.ryan@mcgill.ca; Indra R Gupta; Email: indra.gupta@muhc.mcgill.ca
Submitted: 07/30/2014; Revised: 08/29/2014; Accepted: 09/04/2014
http://dx.doi.org/10.4161/21688362.2014.964547

Data from microarray, SAGE expression profiling, RT-PCR and immunohistochemical analyses of embryonic kidneys have shown that a number of claudins are expressed during kidney development in the mouse and in the rat.[5-12] Gene expression microarray analysis of mRNA isolated from ureteric bud and metanephric mesenchyme of embryonic rats demonstrated that Claudin-3 and -9 mRNA transcripts were strongly upregulated in ureteric bud when compared to metanephric mesenchyme by a factor of 12.5 and 19.1 fold, respectively.[7] Similarly, Schwab *et al.* observed that Claudin-3, -4, -7, and -8 were strongly upregulated in E11.5 mouse ureteric bud when compared to metanephric mesenchyme.[6] Ohta demonstrated that a number of claudins are expressed in the developing mouse kidney and showed that Claudin-3, -4, and -8 appear to be expressed in collecting duct tubules that are derived from the ureteric bud.[9]

The presence of claudins prior to the formation of a urinary filtrate suggested that they could have specific roles during kidney development not related to paracellular transport. In this study, we confirmed by RT-PCR and sequencing that 23 members of the claudin family are expressed in the E13.5 mouse kidney. We then focused our analysis on Claudin-7, -16 and -19 to determine if they have a role during kidney development. Claudin-7 is highly expressed in the aldosterone-sensitive segments of the distal nephron[13] and when inactivated in the mouse, the mice die at postnatal day 12 from severe dehydration from urinary salt wasting such that a coincident defect in nephron formation could be missed if not considered.[14] Mutations in *CLDN16* and *19* have been associated with a rare autosomal recessive syndrome known as familial hypomagnesaemia with hypercalciuria and nephrocalcinosis (FHHNC) characterized by renal calcium and magnesium wasting that can lead to chronic renal failure in childhood or adolescence.[15-17] The early onset of chronic renal failure in childhood suggests that these patients might have a defect in nephron formation during kidney development in addition to possible loss of nephrons secondary to renal calcium deposition. Here, we report a detailed expression analysis of *Cldn7*, *Cldn16*, and *Cldn19* during mouse kidney development and have examined mouse models lacking either *Cldn7* or *Cldn16* to determine if there is evidence for a defect in kidney development.

Materials and Methods

Animal care. Timed-pregnant CD1 and non-pregnant adult mice (Charles River Laboratories, St. Constant, QC) were euthanized using CO_2 inhalation followed by cervical dislocation at embryonic day (E) 9.5, 11.0, 11.5, 12.5, 13.5, 16.5, postnatal day (P) 1, or adulthood to retrieve embryonic, newborn, or adult kidneys as previously described.[11] Newborn pups were euthanized using decapitation. Whole embryos or metanephric kidneys were dissected in PBS using an M5A stereomicroscope (Wild Leitz, Willowdale, ON). All mice used in these studies were housed in temperature-controlled animal facilities in individual ventilated cages with ad libitum access to food and water. Light cycles for all mice were maintained as 12 hours of light and 12 hours of darkness. The mouse studies were performed in accordance with the rules and regulations of the Canadian Council of Animal Care (AUP #4120) and the Office of Laboratory Animal Welfare in the US. Department of Health and Human Services (AUP#172b).

Cldn7 $^{+/-}$ heterozygous breeders on a C57BL/6J background were used to derive P1 litters. The pups were euthanized and genotyped as described.[14] Transgenic *Cldn16*$^{+/-}$ knockdown mice were derived using a lentiviral construct that contained the pFUGW vector in which the snRNP U6 promoter drives overexpression of an siRNA directed to *Cldn16* and the ubiquitin-C promoter drives expression of green fluorescent protein (GFP).[18] Transgenic *Cldn16*$^{+/-}$ knockdown males on a C57BL/6J background were crossed to C57BL/6J female to derive P1 litters. All pups were euthanized, and transgenic progeny were identified by direct observation of GFP fluorescence using a hand-held GFP flashlight as previously reported.[18]

RT-PCR. Ten E11.5, 12.5, or 13.5 mouse kidneys were pooled and RNA was extracted from 3 different pools using the RNeasy kit (Qiagen). For E16.5 and P1 kidneys, 3 kidneys were pooled for RNA extraction. RNA was treated with RNase-free DNase (Ambion) to degrade any traces of DNA. RT-PCR was performed using the One Step RT-PCR Kit (Qiagen). 2 negative controls were included: in one there was no RNA template, and in the other, the reverse transcriptase enzyme was inactivated. β−actin was used as a positive control for the quality of the RNA used in these reactions. Gene specific primers designed to amplify individual claudin family members are shown in **Table 1**. RT-PCR amplicons were sequenced to confirm their identity.

Whole mount in situ hybridization. In situ hybridization was performed on whole E9.5 and 11.0 mouse embryos and on dissected E12.5, 13.5, 16.5, and P1 mouse kidneys as described.[19] Kidneys from P1 mice were bisected prior to fixation and *in situ* hybridization analysis. All samples were fixed overnight in 4% PFA in PBS at 4°C. cDNA clones for *Cldn7*, *Cldn16, Cldn19,* and *Ret* were generated by RT-PCR amplification of the coding sequences using E15 mouse kidney total RNA as a template. The primers sequences were (5′ to 3′): *Cldn7* forward CCATGGGCCTGGAGATCA CCG, *Cldn7* reverse TCAGACGTAGTCCTTGCGGT, *Cldn16* forward CATATGAAGGATCTTCTTCAGTACG, *Cldn16* reverse TTATACTCTGGTGTCTACAGC, *Cldn19* forward CCATGGCCAACTCGGGCCTCCA, *Cldn19* reverse TTACA-CACCCAGGGGGCCCT and *Ret9* forward GATTACAAG-GATGACGAC and reverse TGAGGTAGACGGTGAGCA. Amplified DNA fragments were sequenced to confirm their identity and then subcloned into vectors. To generate antisense riboprobes for *in situ* hybridization analysis, PCRII-TOPO vector (Invitrogen, Camarillo, CA) encoding mouse *Cldn7* was linearized using BamHI while pSC-A vectors (Strataclone, Agilent Technologies, North Torrey Pines Road La Jolla, CA) encoding mouse *Cldn16* and *Cldn19* were linearized with Sma1, and the mouse *Ret* vector was linearized with BamHI respectively. Digoxigenin (DIG)-labeled UTP probes were generated *in vitro* using SP6 RNA polymerase for *Cldn7* and T3 RNA polymerase for *Cldn16*, *Cldn19* and *Ret*. Anti-DIG antibody conjugated to alkaline phosphatase was used to detect duplexes of DIG-labeled antisense riboprobe hybridized to *claudin* mRNA sequences. Treated samples

Table 1. Claudin Primer Sequences used in RT-PCR

Gene	Size	Name of primer	Sequence (5′ to 3′)
Claudin1	636 bp	mCldn1-`F	CCATGGCCAACGCGGGGCTGC
		mCldn1-R	TCACACATAGTCTTTCCCAC
Claudin2	693 bp	mCldn2-F	CCATGGCCTCCCTTGGCGTCC
		mCldn2-R	CACACATACCCAGTCAGGCTG
Claudin3	657 bp	mCldn3-F	CATATGTCCATGGGCTGG
		mCldn3-R	TCAGACGTAGTCCTTGCGGT
Claudin4	633 bp	mCldn4-F	CCATGGCGTCTATGGGACTAC
		mCldn4-R	TTACACATAGTTGCTGGCGG
Claudin5	420 bp	mCldn5-F	CCATGGGGTCTGCAGCGTTGG
		mCldn5-R	GGCGAACCAGCAGAGCGGCAC
Claudin6	660 bp	mCldn6-F	CCATGGCCTCTACTGGTCTGC
		mCldn6-R	TCACACATAATTCTTGGTGG
Claudin7	689 bp	mCldn7-F	CCATGGCCAACTCGGGCCTGCAAC
		mCldn7-R	TCACACGTATTCCTTGGAGG
Claudin8	678 bp	mCldn8-F	CCATGGCAACCTACGCTCTTC
		mCldn8-R	CTACACATACTGACTTTTGG
Claudin9	654 bp	mCldn9-F	CCATGGCTTCCACTGGCCTTG
		mCldn9-R	TCACACATAGTCCCTCTTATC
Claudin10	689 bp	mCldn10a-F	CCATGTCCAGGGCACAGATCT
		mCldn10b-F	CCATGGGTAGCACGGCCTTGG
	696 bp	mCldn10-R	TTAGACATAGGCATTTTTATC
Claudin11	624 bp	mCldn11-F	CCATGGTAGCCACTTGCCTTC
		mCldn11-R	TTAGACATGGGCACTCTTG
Claudin12	735 bp	mCldn12-F	CCATGGGCTGCCGAGATGTCC
		mCldn12-R	TTAAGTGCTGTGTGAGACTAC
Claudin13	636 bp	mCldn13-F	CCATGGTCGTCAGCAAACAAG
		mCldn13-R	TCAAACATCTAAGGTATCG
Claudin14	720 bp	mCldn14-F	CCATGGCCAGCACAGCGGTCC
		mCldn14-R	TCACACGTAGTCATTCAGCC
Claudin15	684 bp	mCldn15-F	CATATGTCGGTAGCTGTGGAGACC
		mCldn15-R	CTACACGTATGCGTTTTTGC
Claudin16	708 bp	mCldn16-F	CATATGAAGGATCTTCTTCAGTACG
		mCldn16-R	TTATACTCTGGTGTCTACAGC
Claudin17	675 bp	mCldn17-F	CCATGGCTTTTTATCCCTTAC
		mCldn17-R	TTAGACGTAGCTGGTGGAAG
Claudin18	150 bp	mCldn18-F	TTCATCATCTCCGGCATCTG
		mCldn18-R	CAAAGGTGTACCTGGTCTGA
Claudin19	675 bp	mCldn19-F	CCATGGCCAACTCGGGCCTCCA
		mCldn19-R	TTACACACCCAGGGGGCCCT
Claudin20	660 bp	mCldn20-F	ATGGCCTCGGCAGGTCTCC
		mCldn20-R	TTACATGTAATCCTTCAAGTTATG
Claudin22	663 bp	mCldn22-F	CCATGGGCTTAGTCTTCCGAAC
		mCldn22-R	TTAGATTTCTGGATTGGCT
Claudin23	891 bp	mCldn23-F	CATATGCGGACGCCGGTGGTGATGACG
		mCldn23-R	CTACAGGTCGGAGTCACAGG
Claudin24	663 bp	mCldn24-F	CCATGGCTTTCATCTTCAGAACG
		mCldn24-R	TTACACTTTAGGCTGTACAGTTCC
β-actin	336 bp	mβ-actin-F	CACAGCTGAGAGGGAAATC
		mβ-actin-R	TCAGCAATGCCTGGGTAC

were developed using nitro blue tetrazolium chloride, 5-bromo-4-chloro-3-indolyl phosphatase substrate in NTMT. All kidneys were photographed and E16.5 and P1 kidneys were processed for cryosectionning. 15 μm frozen sections from E16.5 and P1 mouse kidneys were counterstained with eosin and coverslipped with glycerol-gelatin aqueous mounting medium (Sigma-Aldrich) for imaging, while earlier time points were imaged as whole mounts.

Immunohistochemistry and immunofluorescence. E16.5, P1, and P28 kidneys from CD1 mice were dissected, fixed in 6:3:1 (ethanol:water:formaldehyde) and processed for paraffin sectioning or cryosectioned for immunofluorescent studies. Mouse anti-Calbindin-D-28K (C9848, Sigma-Aldrich), rabbit anti-Claudin 7 (E10590, Spring Biosciences), rabbit anti-Tamm Horsfall glycoprotein/Uromodulin (BT-590, Biomedical Technologies Inc.), and rabbit anti-Claudin-16 (34–5400, Invitrogen) were used at a 1:200 dilution. Rabbit anti-Claudin-19 antibody was generated by Dr. J. Hou[20] and used at a 1:200 dilution. Hematoxylin QS (Vector Laboratories) was used as a counterstain. Color development was performed using the Vectastain ABC kit (Vector Laboratories). For the immunofluorescent studies, mouse anti-ZO-1 (339100, Invitrogen), mouse anti-Occludin (331500, Invitrogen), rabbit anti-Claudin-16 (34-5400, Invitrogen), and rabbit anti-Claudin-19 (Dr. J. Hou) were used, each at a dilution of 1:50. Alexa Fluor 555 goat anti-mouse (A21127, Invitrogen) and Alexa Fluor 488 goat anti-rabbit (A11008, Invitrogen) were used as secondary antibodies at a concentration of 1:100.

Nephron number assessment. P1 kidneys were dissected from pups derived from *Cldn7*$^{+/-}$ heterozygous matings and transgenic *Cldn16*$^{+/-}$ crosses, fixed in formalin, dehydrated and then paraffin-embedded for sectioning. Total nephron counts were obtained by counting every tenth section as we have done previously. [21] Each kidney was sectioned in its entirety and serial sections of 7 μm thickness were obtained and stained with hematoxylin and eosin. The sections were analyzed using Image J

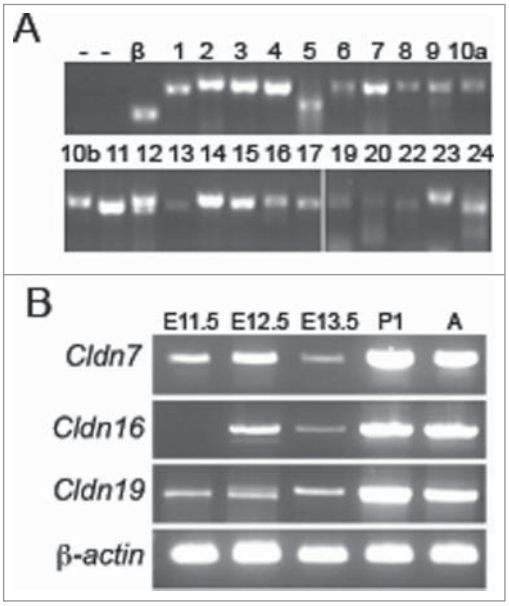

Figure 1. Temporal Expression Analysis of Claudins during Mouse Kidney Development. (**A**) RT-PCR analysis of all claudin family members in E13.5 mouse kidneys. β-actin (β) was used as a positive control and RT-PCR reactions without the addition of RNA (lane 1) or with inactivated reverse transcriptase ('—'; lanes 1 and 2) served as negative controls. The claudin family member is listed above each lane. *Cldn18* was not amplified (data not shown). All RT-PCR amplicons were sequenced to confirm identity. (**B**) RT-PCR analysis of *Cldn7*, *Cldn16*, and *Cldn19* at different stages of kidney development. β-actin was amplified as an internal control. *Cldn7* and *Cldn19* mRNA transcripts are expressed from embryonic day (E) 11.5 onwards, whereas *Cldn16* mRNA transcripts are expressed from E12.5 onwards.

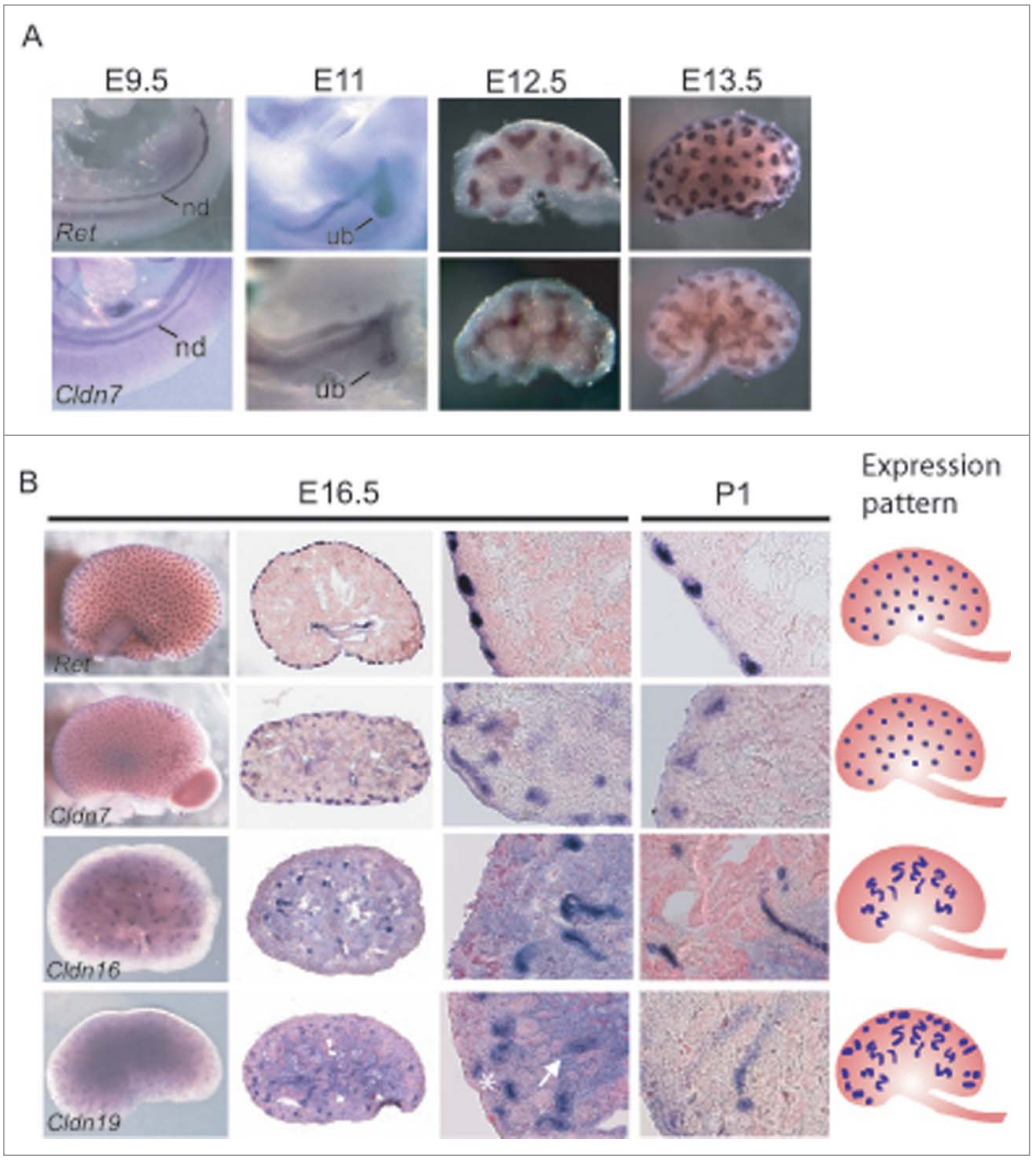

Figure 2. Spatial Expression Analysis of *Cldn7, Cldn16,* and *Cldn19* mRNA Transcripts during Mouse Kidney Development. (**A-B**) Whole mount *in situ* hybridization was performed on whole embryos at embryonic day (E) 9.5 and E11.0, and on whole kidneys at E12.5, E13.5, E16.5, and P1 for *Cldn7, Cldn16, Cldn19*, and *Ret*. E16.5 and P1 kidneys were cryosectioned at 15 μm thickness and counterstained with eosin. *Cldn7* expression is observed in the nephric duct (nd) at E9.5 and in the ureteric bud (ub) at E11.0. At E11.0, E12.5, E13.5 and E16.5 *Cldn7* is seen in the ureteric bud trunks and the tips. At P1, *Cldn7* is detected mostly in ureteric bud tips, similar to *Ret* expression at the same stage. *Cldn16* and *Cldn19* transcripts are first detected at E16.5. *Cldn16* is predominantly expressed in late tubular structures, while *Cldn19* is expressed in both early and late tubular structures that will eventually become the Loop of Henle. On the far right schematic patterns are shown indicating a ureteric bud tip pattern (*Cldn7* and *Ret*), a late tubule pattern (*Cldn16*), and a combined early and late tubule pattern (*Cldn19*) as described.[23]

(v1.36b). Individual glomeruli were identified by the presence of a glomerular tuft with an adjacent Bowman's capsule and were counted using the point selection tool and the auto measure function. Every tenth section was counted, therefore the total nephron number for each kidney was calculated by multiplying this value by 10. The Student's t-test was used for statistical analysis of the data.

Results

Multiple claudins are expressed during mouse kidney development

To determine which claudin family members are expressed during kidney development, we performed RT-PCR analyses using RNA that was extracted from a pool of mouse embryonic kidneys at E13.5, a time point at which both ureteric bud branching morphogenesis and nephrogenesis are well underway. The identity of all PCR products was confirmed by Sanger sequencing. At E13.5, 23 mouse Claudin family members were expressed, including *Cldn7*, *Cldn16*, and *Cldn19* (**Fig. 1A**). Claudin-18 was the only member that was not amplified at this time point. A more detailed expression analysis was performed for *Cldn7*, *Cldn16*, and *Cldn19* to track their temporal expression in the embryonic and postnatal kidney. The analysis revealed that *Cldn7* and *Cldn19* are detected at E11.5, while *Cldn16* was not detected until E12.5 (**Fig. 1B**).

Claudin-7, -16, and -19 are expressed in specific lineages during kidney development

We examined the spatial expression patterns of *Cldn7*, *Cldn16*, and *Cldn19* using *in situ* hybridization at critical stages of kidney development including E9.5 when the nephric duct is well-delineated, E11 when the ureteric bud first emerges from the nephric duct and invades the metanephric mesenchyme and branches, and E12.5 and E13.5, when there is more extensive ureteric bud branching morphogenesis and early nephron precursors are detected. We also examined E16.5 when the glomerulus becomes vascularised and nephron segments begin to differentiate[22] and postnatal day 1 to complete the developmental expression analysis.

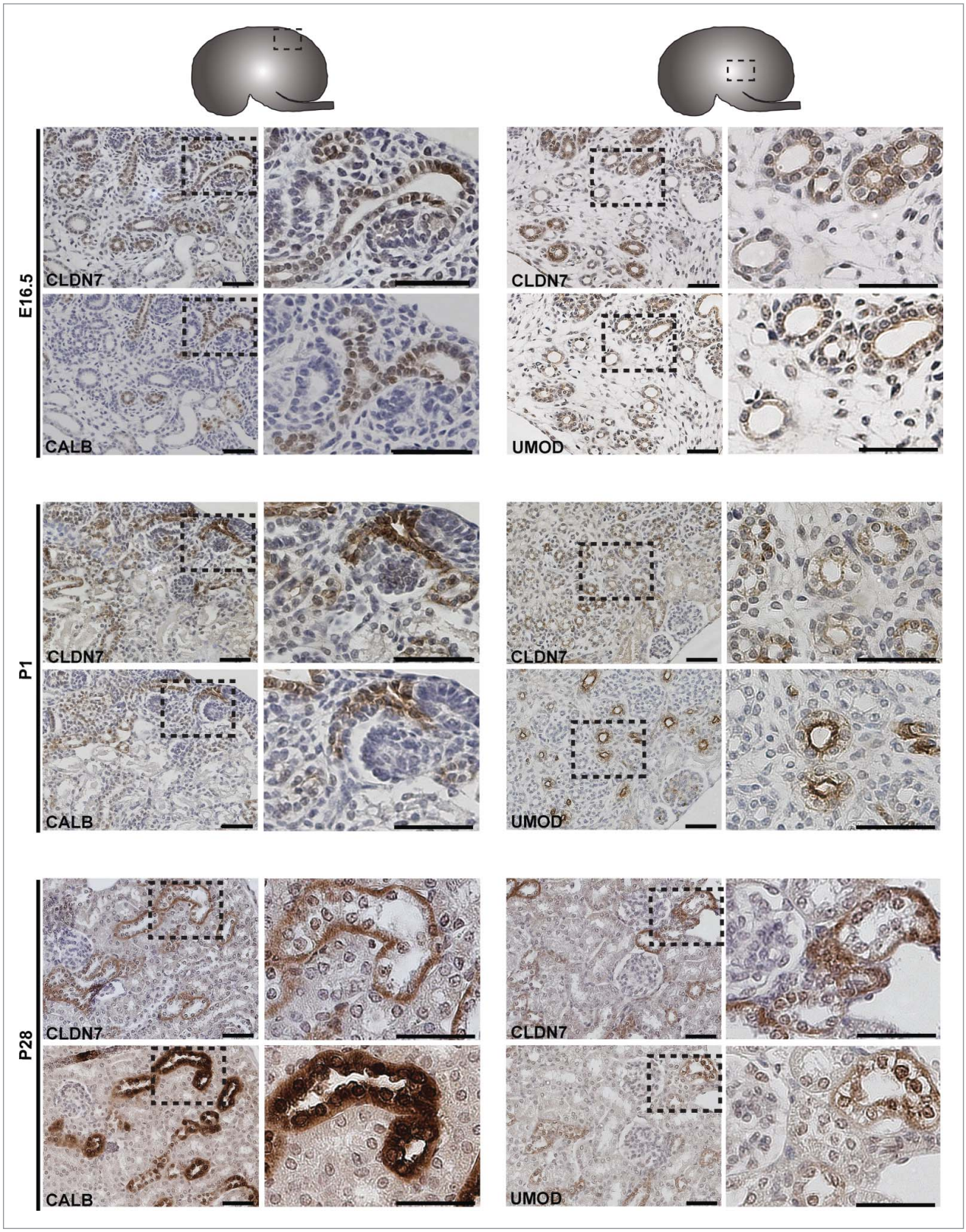

Figure 3. Protein Expression of Claudin-7 during Mouse Kidney Development. Immunohistochemistry was performed on paraffin-embedded sections taken from mouse kidneys at embryonic day (E) 16.5, postnatal day (P) 1 and P28 as shown. Claudin-7 is expressed in ureteric bud trunks and tips at E16.5 and in distal tubular segments as well at P1 and P28, based on its overlapping expression with Calbindin-D-28K and with Uromodulin. A higher magnification of the boxed regions are shown to the right of each image. Scale bar = 50 μm.

Cldn7 was highly expressed within the nephric duct, the emerging ureteric bud, the ureteric bud trunks and the tips, but by P1, it was mostly detected in the ureteric bud tips (**Fig. 2A**,**B**). Whereas *Ret* was limited to the tips of the ureteric bud branches from E12.5-16.5, *Cldn7* was expressed more broadly at the tips as well as in the adjacent ureteric bud trunks. At P1, the expression patterns of *Ret* and *Cldn7* looked more similar with both highly concentrated in the ureteric bud tips.

While *Cldn16* and *Cldn19* were detected by RT-PCR beginning at E12.5 and E11.5 respectively (**Fig. 1B**), whole mount *in situ* hybridization failed to detect any signal for either transcript before E16.5 (data not shown), suggesting that their expression is low. At E16.5, both *Cldn16* and *Cldn19* mRNA transcripts were expressed in late tubular structures, one of 8 discernible patterns recently used to define gene expression profiles during kidney development (**Fig. 2B**).[23] While both transcripts demonstrated this pattern, *Cldn19* transcripts were detected more broadly and were also apparent in early tubular structures. These early and late tubular structures give rise to the Loop of Henle that progresses from an anlage, to a primitive loop, and then to an immature loop prior to its final differentiation.[24-25]

Protein expression was examined by performing immunohistochemistry on paraffin-embedded sections and immunofluorescence on cryosections (**Figs. 3–6**). At E16.5 and at P1, CLDN7 was detected in uroepithelial cells in ureteric bud trunks and tips and appeared to be expressed both apically and basolaterally (**Figs. 3 and 6**). Similar expression was noted at P28, but here CLDN7 was predominantly detected in distal tubular segments based on its overlapping expression with Calbindin-D-28K and with Uromodulin.[24] Calbindin-D-28K protein is expressed by the distal convoluted tubule, the connecting tubule and the collecting duct, while Tamm Horsfall or Uromodulin protein is expressed by the thin and thick ascending limbs of the Loop of Henle.[24] CLDN16 and 19 were strongly expressed in both the primitive and the mature Loop of Henle at E16, P1 and P28 and showed overlapping expression with Uromodulin that also demarcates the Loop of Henle[24] (**Figs. 4 and 5**). CLDN19 showed more broad expression at all stages examined and overlapped with both Calbindin-D-28K and Uromodulin (**Fig. 5**), while CLDN16 did not show overlapping expression with Calbindin-D-28K (data not shown). By immunofluorescence, it was evident that all 3 claudins co-localize with both ZO-1 and with Occludin, confirming their expression in tight junctions (**Fig. 6**).

Nephron number assessment in mouse models lacking Claudin-7 and Claudin-16

Based on their expression patterns during kidney development, we examined mutant mouse models lacking Claudin-7 and Claudin-16 to determine if these mice had defects in nephron formation. Crosses were established between $Cldn7^{+/-}$ breeders[14] and kidneys from the newborn pup offspring were sectioned for histology and total nephron number assessment. Kidney sections from all of the pups including the homozygous

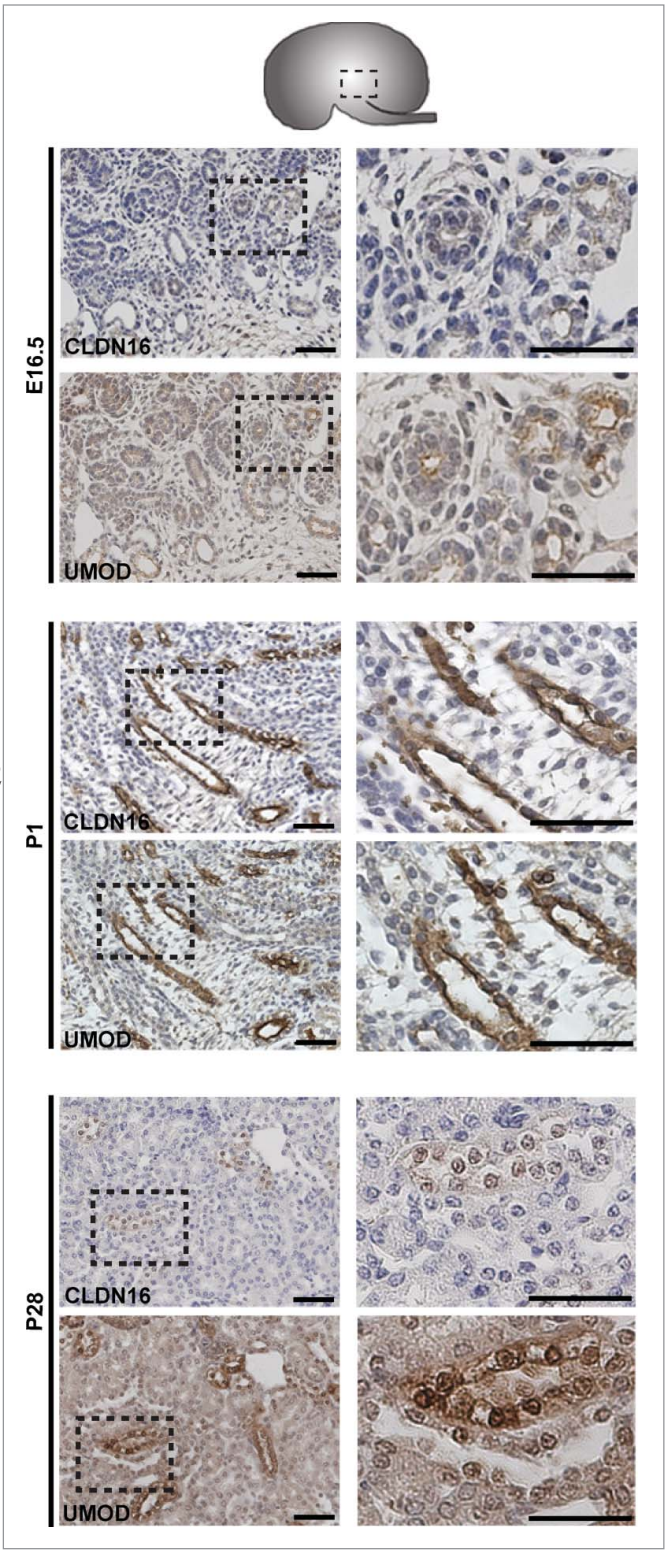

Figure 4. Protein Expression of Claudin-16 during Mouse Kidney Development. Immunohistochemistry was performed on paraffin-embedded sections taken from mouse kidneys at E16.5, P1 and P28 as shown. Claudin-16 is expressed in primitive and mature Loop of Henle tubules as indicated by its overlapping expression with Uromodulin at all stages. A higher magnification of the boxed regions are shown to the right of each image. Scale bar = 50 μm.

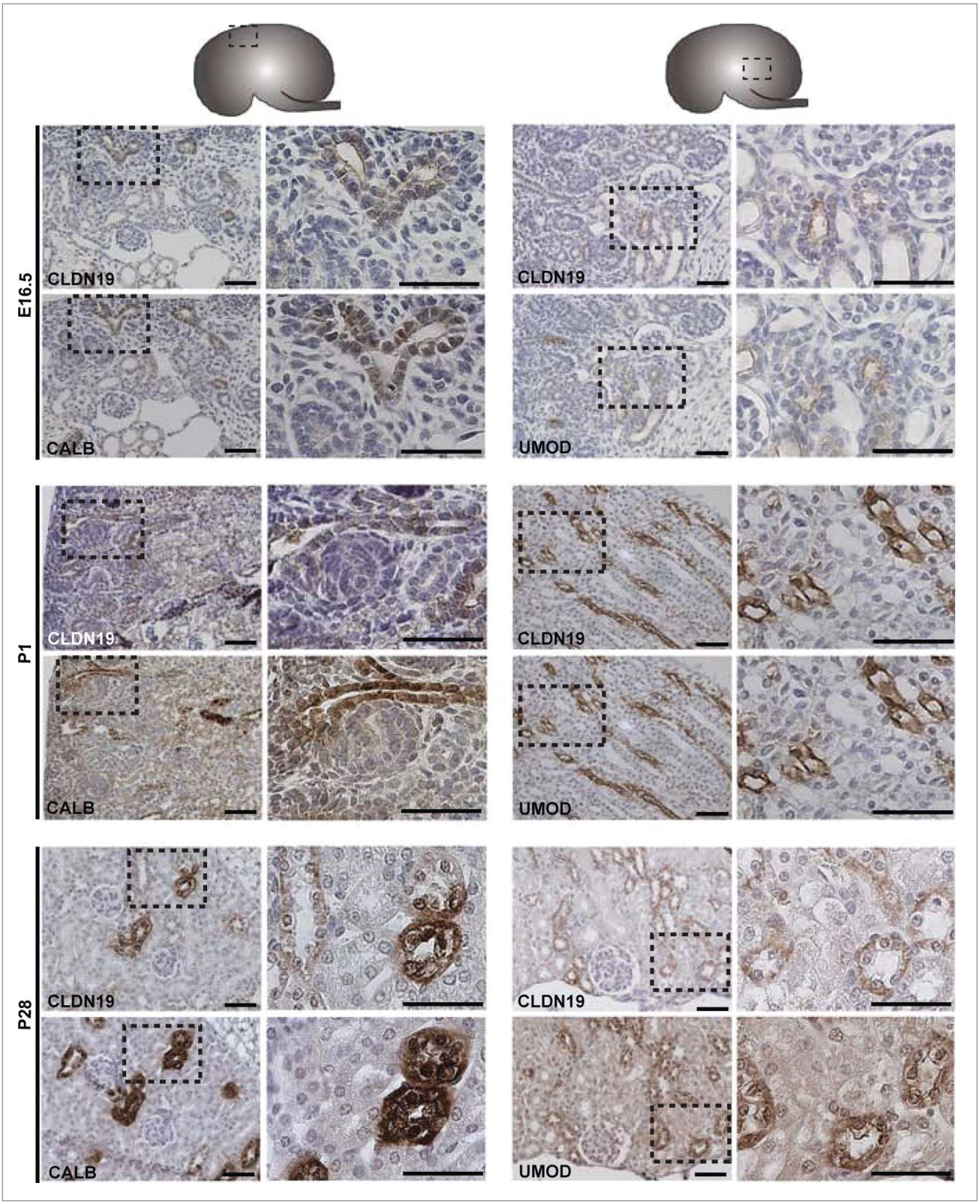

Figure 5. Protein Expression of Claudin-19 during Mouse Kidney Development. Immunohistochemistry was performed on paraffin-embedded sections taken from mouse kidneys at E16.5, P1 and P28 as shown. Claudin-19 is expressed in primitive and mature Loop of Henle tubules as indicated by its overlapping expression with Uromodulin at all stages. Claudin-19 shows broader expression than Claudin-16 and also overlaps with Calbindin-D-28K. A higher magnification of the boxed regions are shown to the right of each image and show regions of overlap with Uromodulin or Calbindin-D-28K. Scale bar = 50 μm.

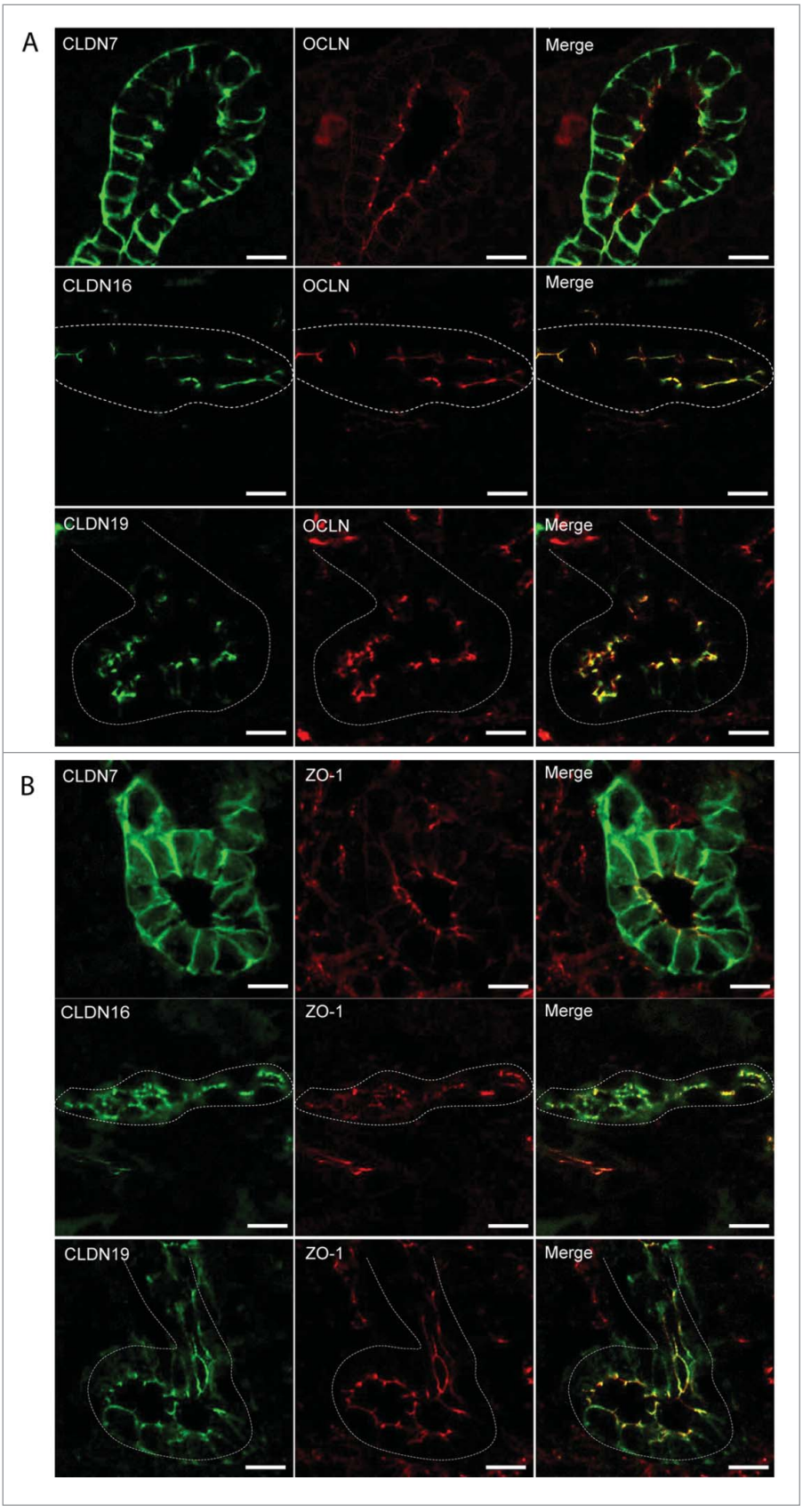

Figure 6. Claudin-7, 16, and -19 Co-Localize with Tight Junction Markers. Immunofluorescence was performed on cryosections taken from mouse P1 kidneys using antibodies to Claudin-7, -16, and -19 and co-localization was performed using antibodies to 2 tight junction markers, Occludin (**A**), and ZO-1 (**B**). Claudin-7 is expressed apically and basolaterally in ureteric bud tubules and is co-expressed with both ZO-1 and Occludin. Claudin-16 is expressed apically in Loop of Henle tubules and is co-expressed with ZO-1 and Occludin. Claudin-19 is expressed apically in Loop of Henle tubules and is co-expressed with ZO-1 and Occludin. Dotted white lines outline tubule segments. Scale bar = 10 μm.

and heterozygous mutants appeared grossly normal with no defects noted in the extent of ureteric bud branching morphogenesis or in the organization of the cortex and the medulla. There was no significant difference in nephron number noted in kidneys when comparing wildtype to heterozygous or to homozygous null pups (**Fig. 7A**, mean nephron number +/− SD; wt: 5160 ± 872 vs. heterozygous: 5099 ± 1312 vs. null: 4648 ± 656, n = 7 kidneys/group $P > 0.05$).

A similar analysis was performed on transgenic *Cldn16*$^{+/-}$ knockdown newborn pups that were derived using RNAi[18] to determine if they exhibited any evidence of a renal malformation. Kidney sections from wildtype and transgenic *Cldn16* knockdown pups appeared grossly normal. Assessment of nephron number revealed no differences when comparing wildtype and transgenic knockdown pups (**Fig. 7B**, mean nephron number +/− SD; wt: 5220 ± 1328 vs. knockdown: 5682 ± 2011, n = 8 kidneys/group $P > 0.05$).

Discussion

Our data demonstrate that 23 mouse claudin family members are expressed during embryonic kidney development and that Claudin-7, -16, and -19 have specific and distinct expression patterns. Despite Claudin-7's expression within the ureteric bud lineage and Claudin-16's expression within renal tubules, we noted that neither of the mouse models lacking these claudins showed evidence of renal maldevelopment nor did they

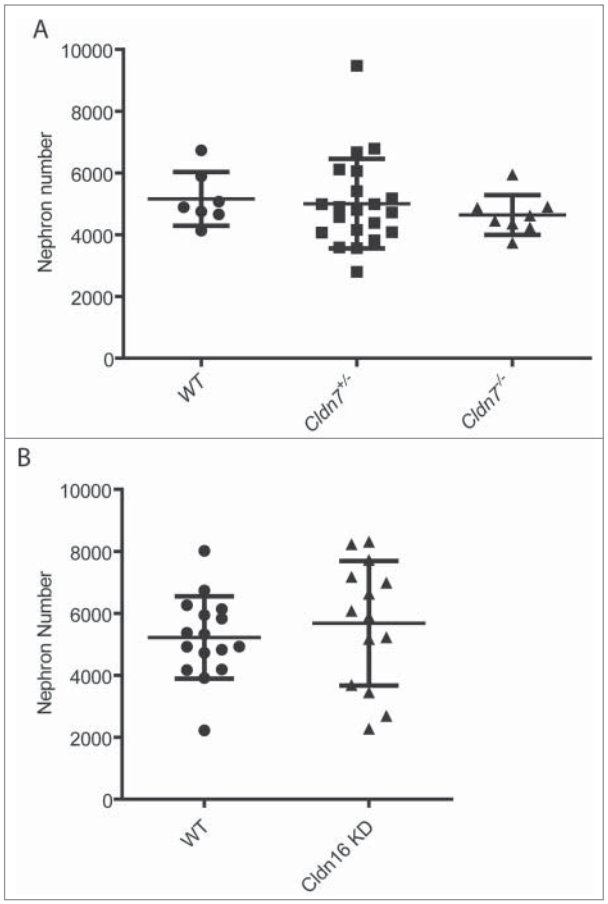

Figure 7. Nephron Number in Mouse Models with Mutations in Claudin-7 and Claudin-16. P1 kidneys were paraffin-embedded and sectioned and stained with hematoxylin and eosin for nephron number counts. (**A**) Total nephron number for the right kidney for each pup was calculated from 6 litters and mean values +/− SD are shown. Kidneys from *Cldn7* −/− pups do not have fewer nephrons (n = 11 kidneys; 4648 ± 656 nephrons/kidney) compared to kidneys from wildtype pups (n = 7; 5160 ± 872 nephrons/kidney, p = 0.174) or when compared to kidneys from heterozygous pups (n = 27 kidneys; 5099 ± 1312 nephrons/kidney, p = 0.287). (**B**) Total nephron number for both kidneys for each pup was calculated from 1 litter and mean values +/− SD are shown. Kidneys from *Cldn-16* +/− knockdown pups do not have fewer nephrons (n = 14; 5682 ± 2011 nephrons/kidney) compared to kidneys from wildtype pups (n = 16 kidneys; 5220 ± 1328 nephrons/kidney, p = 0.458).

demonstrate a deficit in nephron number. We therefore speculate that other claudin family members can compensate for a lack of Claudin-7 and Claudin-16 during kidney development.

During the emergence of the ureteric bud and the subsequent steps of branching morphogenesis, individual cells undergo cell shape changes to elicit the formation of buds and branch points, although the forces that lead to these changes are not well-characterized.[26] The purse-string hypothesis suggests that constriction of actin filaments on one side of an epithelial cell will change its shape from columnar to triangular or wedge-shaped,[27-28] and this has been proposed as a mechanism by which buds and branch points might form during ureteric bud branching morphogenesis.[10] The claudin family of proteins are expressed within epithelial tight junction complexes and are sufficient for the formation of tight junction strands when ectopically expressed in fibroblasts.[29] The ureteric bud and its derivatives have tight junctions based on electron microscopic images.[11] We therefore speculate that claudin proteins that are expressed in the ureteric bud lineage, including CLDN3, CLDN4, CLDN7, CLDN8, and CLDN9,[10,11] may influence cell shape change during ureteric bud branching morphogenesis via their C-terminal tails that interact with PDZ domain adaptor proteins, like ZO-1 and MUPP1, to link tight junctions to the actin cytoskeleton.[3]

Claudin-16 and Claudin-19 are expressed at later stages of renal development in tubular segments that arise when the metanephric mesenchyme undergoes mesenchymal-to-epithelial transition. Their expression patterns resemble that of Pou3f3 (Brn1)[25] and Uromodulin[24] such that taken together they define a molecular network that specifies the Loop of Henle. Claudin-19 has a broader expression pattern than Claudin-16 showing overlapping expression with both Calbindin-D-28K and Uromodulin, suggesting that in addition to its expression in the Loop of Henle, it is expressed within the distal convoluted tubule and the connecting tubule. A similar expression pattern for Claudin-19 has been shown by Lee *et al.* using a different antibody raised to amino acids 23–39.[30]

Our analysis of Claudin-7 and Claudin-16 deficient mouse models suggests that these 2 members are not essential for kidney development. These studies do not eliminate the possibility that they participate in the development and differentiation of the nephrons and the collecting duct network, however other claudin family members may be able to compensate for their absence. Remarkably, many of the single claudin loss-of-function mouse models exhibit very subtle physiological phenotypes that are more restricted than their expression domains.[3] In fact, very few claudin mutations lead to abnormal renal physiology, in spite of the fact that most claudins are expressed within the adult nephron.[13,31,32] This strongly suggests that claudins may function in combination with other claudins to exert their effects on paracellular transport. There is evidence that claudins can both heteromerize and homomerize within tight junctions to influence paracellular transport,[33] but thus far a deeper understanding of how this influences cell and tissue function remains elusive.

So the question remains, why are so many claudins expressed in the embryonic kidney? While it is possible that their only function is to establish the paracellular barrier, we hypothesize that they are required for MET and branching morphogenesis during nephron differentiation and establishment of the collecting duct network. We propose that the absence of a renal developmental phenotype following removal of a single claudin is due to functional redundancy. Therefore, future studies will need to consider knockdown of multiple claudins in combination to begin to elucidate their roles during renal development.

Disclosure of Potential Conflicts of Interest

There were no conflicts of interest to disclose.

Funding

This work was supported by an operating grant from the Kidney Foundation of Canada (IRG and AKR). IRG holds a salary award from the Fonds de la Recherche en Santé du Québec. AKR and IRG are members of the Research Institute of the McGill University Health Center, which is supported in part by the FRSQ.

References

1. Krause G, Winkler L, Mueller SL, Haseloff R F, Piontek J, Blasig I E. Structure and function of claudins. Biochim Biophys Acta 2008; 1778:631; PMID:18036336; http://dx.doi.org/10.1016/j.bbamem.2007.10.018
2. Lal-Nag M, Morin PJ. The claudins. Genome Biol 2009; 10:235; PMID:19706201; http://dx.doi.org/10.1186/gb-2009-10-8-235
3. Gupta IR, Ryan AK. Claudins: unlocking the code to tight junction function during embryogenesis and in disease. Clin Genet 2010; 77:314; PMID:20447145; http://dx.doi.org/10.1111/j.1399-0004.2010.01397.x
4. Costantini F. Genetic controls and cellular behaviors in branching morphogenesis of the renal collecting system. Wiley Interdiscip Rev Dev Biol 2012; 1:693; PMID:22942910; http://dx.doi.org/10.1002/wdev.52
5. Schmidt-Ott KM, Yang J, Chen X, Wang H, Paragas N, Mori K, Li J Y, Lu B, Costantini F, Schiffer M et al. Novel regulators of kidney development from the tips of the ureteric bud. J Am Soc Nephrol 2005; 16:1993; PMID:15917337; http://dx.doi.org/10.1681/ASN.2004121127
6. Schwab K, Patterson L, Aronow B, Luckas R, Liang H-C, Potter S. A catalogue of gene expression in the developing kidney. Kidney Int 2003; 64:1588; PMID:14531791; http://dx.doi.org/10.1046/j.1523-1755.2003.00276.x
7. Stuart RO, Bush KT, Nigam SK. Changes in gene expression patterns in the ureteric bud and metanephric mesenchyme in models of kidney development. Kidney Int 2003; 64:1997; PMID:14633122; http://dx.doi.org/10.1046/j.1523-1755.2003.00383.x
8. Davies JA, Little MH, Aronow B, Armstrong J, Brennan J, Lloyd-MacGilp S, Armit C, Harding S, Piu X, Roochun Y et al.: Access and use of the GUDMAP database of genitourinary development. Methods Mol Biol 2012; 886:185; PMID:22639262; http://dx.doi.org/10.1007/978-1-61779-851-1_17
9. Ohta H, Adachi H, Inaba M. Developmental changes in the expression of tight junction protein claudins in murine metanephroi and embryonic kidneys. J Vet Med Sci 2006; 68:149; PMID:16520537; http://dx.doi.org/10.1292/jvms.68.149
10. Meyer TN, Schwesinger C, Bush KT, Stuart RO, Rose DW, Shah MM, Vaughn DA, Steer DL, Nigam SK. Spatiotemporal regulation of morphogenetic molecules during in vitro branching of the isolated ureteric bud: toward a model of branching through budding in the developing kidney. Dev Biol 2004; 275:44; PMID:15464572; http://dx.doi.org/10.1016/j.ydbio.2004.07.022
11. Haddad N, El Andalousi J, Khairallah H, Yu M, Ryan AK, Gupta IR. The tight junction protein claudin-3 shows conserved expression in the nephric duct and ureteric bud and promotes tubulogenesis in vitro. Am J Physiol Renal Physiol 2011; 301:F1057; PMID:21775479; http://dx.doi.org/10.1152/ajprenal.00497.2010
12. Siddiqui AS, Khattra J, Delaney AD, Zhao Y, Astell C, Asano J, Babakaiff R, Barber S, Beland J, Bohacec S et al. A mouse atlas of gene expression: large-scale digital gene-expression profiles from precisely defined developing C57BL/6J mouse tissues and cells. Proc Natl Acad Sci U S A 2005; 102:18485; PMID:16352711; http://dx.doi.org/10.1073/pnas.0509455102
13. Li WY, Huey CL, Yu AS. Expression of claudin-7 and -8 along the mouse nephron. Am J Physiol Renal Physiol 2004; 286:F1063; PMID:14722018; http://dx.doi.org/10.1152/ajprenal.00384.2003
14. Tatum R, Zhang Y, Salleng K, Lu Z, Lin JJ, Lu Q, Jeansonne BG, Ding L, Chen YH. Renal salt wasting and chronic dehydration in claudin-7-deficient mice. Am J Physiol Renal Physiol 2010; 298:F24; PMID:19759267; http://dx.doi.org/10.1152/ajprenal.00450.2009
15. Simon DB, Lu Y, Choate KA, Velazquez H, Al-Sabban E, Praga M, Casari G, Bettinelli A, Colussi G, Rodriguez-Soriano J et al. Paracellin-1, a renal tight junction protein required for paracellular Mg2+ resorption. Science 1999; 285:103; PMID:10390358; http://dx.doi.org/10.1126/science.285.5424.103
16. Haisch L, Konrad M. Impaired paracellular ion transport in the loop of Henle causes familial hypomagnesemia with hypercalciuria and nephrocalcinosis. Ann N Y Acad Sci 2012; 1258:177; PMID:22731731; http://dx.doi.org/10.1111/j.1749-6632.2012.06544.x
17. Konrad M, Schaller A, Seelow D, Pandey AV, Waldegger S, Lesslauer A, Vitzthum H, Suzuki Y, Luk JM, Becker C et al. Mutations in the tight-junction gene claudin 19 (CLDN19) are associated with renal magnesium wasting, renal failure, and severe ocular involvement. Am J Hum Genet 2006; 79:949; PMID:17033971; http://dx.doi.org/10.1086/508617
18. Hou J, Shan Q, Wang T, Gomes A S, Yan Q, Paul D L, Bleich M, Goodenough DA. Transgenic RNAi depletion of claudin-16 and the renal handling of magnesium. J Biol Chem 2007; 282:17114; PMID:17442678; http://dx.doi.org/10.1074/jbc.M700632200
19. Acloque H, Wilkinson DG, Nieto MA. In situ hybridization analysis of chick embryos in whole-mount and tissue sections. Methods Cell Biol 2008; 87:169; PMID:18485297; http://dx.doi.org/10.1016/S0091-679X(08)00209-4
20. Gong Y, Renigunta V, Himmerkus N, Zhang J, Renigunta A, Bleich M, Hou J. Claudin-14 regulates renal Ca (+)(+) transport in response to CaSR signalling via a novel microRNA pathway. EMBO J 2012; 31:1999; PMID:22373575; http://dx.doi.org/10.1038/emboj.2012.49
21. Murawski IJ, Maina RW, Gupta IR. The relationship between nephron number, kidney size and body weight in two inbred mouse strains. Organogenesis 2010; 6:189; PMID:21197222; http://dx.doi.org/10.4161/org.6.3.12125
22. Thiagarajan RD, Georgas KM, Rumballe BA, Lesieur E, Chiu HS, Taylor D, Tang DT, Grimmond SM, Little MH. Identification of anchor genes during kidney development defines ontological relationships, molecular subcompartments and regulatory pathways. PLoS One 2011; 6:e17286; PMID:21386911; http://dx.doi.org/10.1371/journal.pone.0017286
23. Yu J, Valerius MT, Duah M, Staser K, Hansard JK, Guo JJ, McMahon J, Vaughan J, Faria D, Georgas K et al. Identification of molecular compartments and genetic circuitry in the developing mammalian kidney. Development 2012; 139:1863; PMID:22510988; http://dx.doi.org/10.1242/dev.074005
24. Georgas K, Rumballe B, Wilkinson L, Chiu H S, Lesieur E, Gilbert T, Little M H. Use of dual section mRNA in situ hybridisation/immunohistochemistry to clarify gene expression patterns during the early stages of nephron development in the embryo and in the mature nephron of the adult mouse kidney. Histochem Cell Biol 2008; 130:927; PMID:18618131; http://dx.doi.org/10.1007/s00418-008-0454-3
25. Nakai S, Sugitani Y, Sato H, Ito S, Miura Y, Ogawa M, Nishi M, Jishage K, Minowa O, Noda T. Crucial roles of Brn1 in distal tubule formation and function in mouse kidney. Development 2003; 130:4751; PMID:12925600; http://dx.doi.org/10.1242/dev.00666
26. Costantini F, Kopan R. Patterning a complex organ: branching morphogenesis and nephron segmentation in kidney development. Dev Cell 2010; 18:698; PMID:20493806; http://dx.doi.org/10.1016/j.devcel.2010.04.008
27. Nagele RG, Bush KT, Kosciuk MC, Hunter ET, Steinberg AB, Lee HY. Intrinsic and extrinsic factors collaborate to generate driving forces for neural tube formation in the chick: a study using morphometry and computerized three-dimensional reconstruction. Brain Res Dev Brain Res 1989; 50:101; PMID:2582601; http://dx.doi.org/10.1016/0165-3806(89)90129-6
28. Baker PC, Schroeder TE. Cytoplasmic filaments and morphogenetic movement in the amphibian neural tube. Dev Biol 1967; 15:432; PMID:6032487; http://dx.doi.org/10.1016/0012-1606(67)90036-X
29. Furuse M, Sasaki H, Fujimoto K, Tsukita S. A single gene product, claudin-1 or -2, reconstitutes tight junction strands and recruits occludin in fibroblasts. J Cell Biol 1998; 143:391; PMID:9786950; http://dx.doi.org/10.1083/jcb.143.2.391
30. Lee NP, Tong MK, Leung PP, Chan VW, Leung S, Tam PC, Chan KW, Lee KF, Yeung WS, Luk JM. Kidney claudin-19: localization in distal tubules and collecting ducts and dysregulation in polycystic renal disease. FEBS Lett 2006; 580:923; PMID:16427635; http://dx.doi.org/10.1016/j.febslet.2006.01.019
31. Kiuchi-Saishin Y, Gotoh S, Furuse M, Takasuga A, Tano Y, Tsukita S. Differential expression patterns of claudins, tight junction membrane proteins, in mouse nephron segments. J Am Soc Nephrol 2002; 13:875; PMID:11912246
32. Reyes JL, Lamas M, Martin D, del Carmen Namorado M, Islas S, Luna J, Tauc M, Gonzalez-Mariscal L. The renal segmental distribution of claudins changes with development. Kidney Int 2002; 62:476; PMID:12110008; http://dx.doi.org/10.1046/j.1523-1755.2002.00479.x
33. Angelow S, Ahlstrom R, Yu AS. Biology of claudins. Am J Physiol Renal Physiol 2008; 295:F867; PMID:18480174; http://dx.doi.org/10.1152/ajprenal.90264.2008